

Hypomorphic function and somatic reversion of DOCK8 cause combined immunodeficiency without hyper-IgE

Anne-Kathrin Kienzler,¹ Pauline A van Schouwenburg,¹ John Taylor,² Ishita Marwah,¹ Richa U Sharma,¹ Charlotte Noakes,² Kate Thomson,² Ross Sadler,³ Shelley Segal,⁴ Berne Ferry,³ Jenny C Taylor,⁵ Edward Blair,⁶ Helen Chapel,¹ Smita Y Patel¹

¹Nuffield Department of Medicine, Experimental Medicine Division, University of Oxford, UK
and Oxford NIHR Biomedical Research Centre, John Radcliffe Hospital, Oxford, UK

²Oxford NHS Regional Molecular Genetics Laboratory, Oxford University Hospitals NHS
Trust, Oxford, UK

³Department of Clinical Laboratory Immunology, Churchill Hospital, Oxford University
Hospitals NHS Trust, Oxford, UK

⁴Department of Paediatrics, Children's Hospital, Oxford University NHS Hospitals Trust,
Oxford, UK

⁵Oxford Biomedical Research Centre, Wellcome Trust Centre for Human Genetics, Oxford,
UK

⁶Department of Clinical Genetics, Churchill Hospital, Oxford University NHS Hospitals Trust,
Oxford, UK

Corresponding author:

Anne-Kathrin Kienzler, PhD

University of Oxford

NDM Experimental Medicine and BRC Translational Immunology Laboratory

John Radcliffe Hospital, Level 7, Room 7400

Headley Way

Oxford, OX3 9DU, UK

Email: anne-kathrin.kienzler@ndm.ox.ac.uk

Phone: +44 (0) 1865 857620

Conflict of interest statement:

None of the authors has any potential financial conflict of interest related to this manuscript.

Funding:

This work was supported by the Oxford Partnership Comprehensive Biomedical Research Centre with funding from the Department of Health's National Institute of Health Research (NIHR) Biomedical Research Centre funding scheme. The views expressed in this publication are those of the authors and not necessarily those of the Department of Health. B.F. was supported by the NIHR Chief Scientist Funding.

Word count: 2850

Keywords

DOCK8; combined immunodeficiency; whole exome sequencing; Hyper-IgE syndrome;
phenotypic variability

Abbreviations

CFSE	Carboxyfluorescein diacetate, succinimidyl ester
DHR1/2	DOCK homology region
DOCK8	Dedicator of cytokinesis 8
EBV	Epstein-Barr-Virus
HC	Healthy control
Mut	Mutated DOCK8 transcript (referring to c.6019dupT)
PBMC	Peripheral blood mononuclear cell
PHA	Phytohaemagglutinin
Pt	Patient
Trunc	Truncated DOCK8 protein

Highlights

- Whole exome sequencing identified the underlying defect in a patient with combined immunodeficiency.
- A novel compound heterozygous DOCK8 mutation was identified.
- Expression of a truncated DOCK8 protein with hypomorphic function was identified.
- Somatic reversion of *DOCK8* mainly in T cells was identified.
- DOCK8 deficiency may present without severe viral infections and increased serum IgE levels.

Abstract

Loss-of-function mutations in DOCK8 are linked to hyper-IgE syndrome. Patients typically present with recurrent sinopulmonary infections, severe cutaneous viral infections, food allergies and elevated serum IgE. Although patients may present with a spectrum of disease-related symptoms, molecular mechanisms explaining phenotypic variability in patients are poorly defined. Here we characterized a novel compound heterozygous mutation in *DOCK8* in a patient diagnosed with primary combined immunodeficiency which was not typical of classical DOCK8 deficiency. In contrast to previously identified mutations in *DOCK8* which result in complete loss of function, the newly identified single nucleotide insertion results in expression of a truncated DOCK8 protein. Functional evaluation of the truncated DOCK8 protein revealed its hypomorphic function. In addition we found somatic reversion of *DOCK8* predominantly in T cells. The combination of somatic reversion and hypomorphic DOCK8 function explains the milder and atypical phenotype of the patient and further broadens the spectrum of DOCK8-associated disease.

1. Introduction

Bi-allelic loss-of-function mutations in the guanine-nucleotide exchange factor dedicator of cytokinesis 8 (*DOCK8*) cause autosomal recessive hyper-IgE syndrome. The vast majority of *DOCK8*-deficient patients present with combined immunodeficiency characterized by recurrent sino-pulmonary and/or gastrointestinal infections, severe cutaneous viral infections, severe atopy, eosinophilia and massively elevated serum IgE levels. Patients also have a predisposition to cancer. (1, 2)

Recent studies have highlighted the phenotypic variability of patients suffering from *DOCK8*-deficiency. (3, 4) Patients with susceptibility to infection but less severe allergic disease were identified to carry a functional wild-type *DOCK8* allele in lymphocyte subpopulations due to somatic reversion of the mutated *DOCK8* alleles. (3)

Here we report for the first time a patient with a hypomorphic mutation in *DOCK8* presenting with recurrent bacterial infections, low serum IgM and IgG, CD4 lymphopenia and severely impaired vaccination responses, but without severe viral infections and severe atopy.

2. Methods

Detailed information can be found in the Supplementary Data.

We submitted the variants identified in DOCK8 to be made publically available by ClinVar (<http://www.ncbi.nlm.nih.gov/clinvar/>). The accession numbers are SCV000257461 (deletion chr9:204193-343954), SCV000257462 (c.65C>T), SCV000257463 (c.289C>A), SCV000257464 (c4107C>G), SCV000257465 (c.5433G>A), and SCV000257466 (c.6019dupT).

3. Case presentation

The female patient is the only child of non-consanguineous, healthy parents. She presented aged eight with a two-year history of recurrent bacterial chest infections and radiological signs of early bronchiectasis. The patient also had a long-standing history of mild eczema and asthma requiring treatment with inhaled corticosteroids and beta-agonists. All routine childhood immunizations were received uneventfully. Immunological evaluation (Table I) revealed low serum IgM, normal IgA and IgE, and borderline-low IgG levels which dropped significantly over 12 months. Measurement of responses to previous immunizations demonstrated protective levels of IgG to tetanus toxoid but absent IgG to *Haemophilus influenzae type b*, pneumococcal polysaccharides and measles. Also, despite a history of a normal course of chicken-pox, varicella zoster virus IgG was undetectable. Lymphocyte subset analysis demonstrated low CD4⁺ T cell numbers and low frequencies of CD27⁺ effector B cells (Table I). Following the failure of antibiotic prophylaxis alone to reduce the infection burden, immunoglobulin replacement therapy was commenced with a good clinical response. Sequence analysis of recombination-activating gene (*RAG*) 1, *RAG2*, and DNA cross-link repair 1C (*DCLRE1C* encoding Artemis) did not reveal any mutations. Therefore the patient was given a diagnosis of undefined primary combined immunodeficiency.

4. Results and Discussion

To identify the underlying disease cause, we undertook whole exome sequencing (WES) on the patient and both parents. A novel heterozygous frameshift variant was detected in *DOCK8* in the patient and her mother. Sanger sequencing confirmed a single-nucleotide duplication [c.6019dupT (p.Tyr2007Leufs*12)] within the conserved DOCK homology region 2 (DHR2) domain of *DOCK8*, leading to a frameshift and premature stop-codon (Figure 1, A and C, and Supplementary Table 1]. As autosomal recessive mutations in *DOCK8* cause combined immunodeficiency, we screened for further variants in *DOCK8*. Analysis of single nucleotide polymorphisms (SNPs) across *DOCK8* in the trio revealed apparent loss of paternal contribution of two SNPs in a 5' region of the gene (Supplementary Table 1), indicating the possibility of a paternally inherited deletion. Array comparative genomic hybridization analysis confirmed a large deletion encompassing exons 1-14 of *DOCK8* in the patient and her father (approx. 140kb deletion of 9p24.3, base pair 204,193 to 343,954) (Figure 1, B and C). This novel compound heterozygous mutation in *DOCK8* was the only disease-causing variant identified in the patient (Supplementary Tables 2-4).

The deletion in *DOCK8* is predicted to result in absence of any protein expression since the deletion includes the start codon. The frameshift mutation is predicted to result in the production of a truncated protein lacking 81 amino acids (~11kDa). Indeed, patient EBV cells expressed low amounts of a truncated DOCK8 protein, but not the full-length protein (Figure 1D). We hypothesized that this truncated DOCK8 protein has hypomorphic function accounting for the milder clinical presentation of our patient.

Previous studies of DOCK8-deficient patients report impaired T cell proliferation. (1, 2) At the age of ten years, both CD4⁺ and CD8⁺ patient T cells did not proliferate in response to mitogen (PHA) stimulation (Figure 2A), consistent with an inability of the truncated DOCK8 protein to transmit proliferative signals. Interestingly, when studying T cell proliferation at the time of WES (four years later), proliferation of both CD4⁺ and CD8⁺ patient T cells was present, although reduced compared to a healthy control (Figure 2B). We hypothesized that this difference in T cell proliferation could be explained by somatic reversion of *DOCK8*. Indeed, Sanger sequencing of *DOCK8* cDNA of T cells and subsequent peak height quantification revealed that two thirds of all *DOCK8* transcripts are wild-type (Figure 2C), showing somatic reversion of *DOCK8* as previously described. (3) Somatic reversion of *DOCK8* in T cells was confirmed by pyrosequencing of *DOCK8* (Figure 2D). Therefore improved T cell proliferation over time is likely to be due to somatic reversion of *DOCK8* in patient T cells.

The frequency of somatic reversion in B cells was half compared to the *DOCK8* reversion in T cells (Figure 2D) indicating a higher proportion of B cells expressing only the truncated DOCK8. Interestingly, patient CD19⁺ B cells immortalized with EBV expressed only mutated *DOCK8* transcripts (Figure 2E) suggesting selective outgrowth of cells that did not undergo somatic reversion. As migration of DOCK8-deficient B cells has previously been shown to be impaired (5), we investigated functionality of the truncated DOCK8 protein in a transwell assay using the patient EBV B cells expressing only the truncated version of DOCK8. Migration of patient EBV B cells was comparable to EBV B cell lines of healthy controls and significantly better than that of EBV B cells of a patient with complete loss-of-function mutation in DOCK8 (*DOCK8*^{null}) (Figure 2F). This shows that migration was not significantly affected by the truncation of the DOCK8 protein.

DOCK8 is a large protein with at least two described functional domains, the N-terminal DOCK homology region (DHR) 1 domain and the C-terminal DHR2 domain. There is only little data available on which downstream cellular functions are mediated by each domain. Our data showing normal migration of patient EBV cells expressing a truncated DOCK8 protein in which the C-terminal DHR2 domain is disrupted suggest that this domain is dispensable for lymphocyte migration. In line, Ham et al. (6) showed that the N-terminal region of DOCK8, but not the C-terminal region of DOCK8 is a crucial binding site for Wiskott–Aldrich syndrome protein (WASp), a protein involved in actin cytoskeleton remodelling and migration.

The C-terminal DHR2 domain of DOCK8 exhibits the guanine nucleotide exchange in the small GTPase cell division control protein 42 homolog (CDC42). To our knowledge it is not yet clear which cellular functions are modulated by signalling events initiated by the DOCK8-mediated guanine nucleotide exchange. Absent T cell proliferation when the patient presented initially in clinic, presumably before somatic reversion took place, suggests that lymphocyte proliferation is likely modulated by the guanine nucleotide exchange function in the DHR2 domain. Further in-depth characterization of truncated DOCK8 proteins will provide a valuable tool for gaining a better understanding of the function of DOCK8 in immune regulation and genotype-phenotype correlations in various patients with DOCK8 deficiencies.

Currently, curative hematopoietic stem cell transplantation (HSCT) is the definitive treatment for DOCK8 deficiency. Without HSCT, infections and an increased risk of developing malignancies due to impaired clearance of oncogenic viruses are life-threatening complications associated with DOCK8 deficiency. HSCT is expected to prevent both;

however there is no data available on the development of malignancies post HSCT. In our patient, expression of truncated, partially functional DOCK8 in combination with somatic reversion in T cells is sufficient to maintain antiviral immunity, as shown by the absence of severe viral infections. Therefore, the risk versus benefit of HSCT is unclear in patients with less severe disease and demands careful consideration.

Conclusion

Here we reported a patient with atypical DOCK8 deficiency characterized by a much milder phenotype of the immunodeficiency compared to classical DOCK8 deficiency which further broadens the spectrum of DOCK8 associated diseases. As suggested by normal patient EBV B cell migration and initially absent T cell proliferation in addition to somatic reversion of *DOCK8* predominantly in T cells, this relatively mild phenotype is the result of hypomorphic DOCK8 function and somatic reversion.

Acknowledgements

We thank Dr V. Lougaris for providing the EBV line of a patient with DOCK8 loss-of-function mutation. We thank Dr. F. Dhalla for help in clinical care and sample collection. We thank Dr D.F. Kelly for critical reading of the manuscript. We thank the members of the Clinical Immunology Laboratory at Great Ormond Street Hospital for their contribution to the immunological characterization of the patient. We thank the patient and her family for their support and cooperation. This work was supported by the Oxford Partnership Comprehensive Biomedical Research Centre with funding from the Department of Health's National Institute of Health Research (NIHR) Biomedical Research Centre funding scheme. The views expressed in this publication are those of the authors and not necessarily those of the Department of Health. B.F. was supported by the NIHR Chief Scientist Funding.

References

1. Engelhardt, K.R., McGhee, S., Winkler, S., Sassi, A., Woellner, C., Lopez-Herrera, G., Chen, A., Kim, H.S., Lloret, M.G., Schulze, I., et al. 2009. Large deletions and point mutations involving the dedicator of cytokinesis 8 (DOCK8) in the autosomal-recessive form of hyper-IgE syndrome. *J Allergy Clin Immunol* 124:1289-1302 e1284.
2. Zhang, Q., Davis, J.C., Lamborn, I.T., Freeman, A.F., Jing, H., Favreau, A.J., Matthews, H.F., Davis, J., Turner, M.L., Uzel, G., et al. 2009. Combined immunodeficiency associated with DOCK8 mutations. *N Engl J Med* 361:2046-2055.
3. Jing, H., Zhang, Q., Zhang, Y., Hill, B.J., Dove, C.G., Gelfand, E.W., Atkinson, T.P., Uzel, G., Matthews, H.F., Mustillo, P.J., et al. 2014. Somatic reversion in dedicator of cytokinesis 8 immunodeficiency modulates disease phenotype. *J Allergy Clin Immunol* 133:1667-1675.
4. Ruiz-Garcia, R., Lermo-Rojo, S., Martinez-Lostao, L., Mancebo, E., Mora-Diaz, S., Paz-Artal, E., Ruiz-Contreras, J., Anel, A., Gonzalez-Granado, L.I., and Allende, L.M. 2014. A case of partial dedicator of cytokinesis 8 deficiency with altered effector phenotype and impaired CD8(+) and natural killer cell cytotoxicity. *J Allergy Clin Immunol* 134:218-221.
5. Sic, H., Kraus, H., Madl, J., Flittner, K.A., von Munchow, A.L., Pieper, K., Rizzi, M., Kienzler, A.K., Ayata, K., Rauer, S., et al. 2014. Sphingosine-1-phosphate receptors control B-cell migration through signaling components associated with primary immunodeficiencies, chronic lymphocytic leukemia, and multiple sclerosis. *J Allergy Clin Immunol* 134:420-428.
6. Ham, H., Guerrier, S., Kim, J., Schoon, R.A., Anderson, E.L., Hamann, M.J., Lou, Z., and Billadeau, D.D. 2013. Dedicator of cytokinesis 8 interacts with talin and Wiskott-Aldrich syndrome protein to regulate NK cell cytotoxicity. *J Immunol* 190:3661-3669.
7. Piatosa, B., Wolska-Kusnierz, B., Pac, M., Siewiera, K., Galkowska, E., and Bernatowska, E. 2010. B cell subsets in healthy children: reference values for evaluation of B cell maturation process in peripheral blood. *Cytometry B Clin Cytom* 78:372-381.
8. Shearer, W.T., Rosenblatt, H.M., Gelman, R.S., Oyomopito, R., Plaeger, S., Stiehm, E.R., Wara, D.W., Douglas, S.D., Luzuriaga, K., McFarland, E.J., et al. 2003. Lymphocyte subsets in healthy children from birth through 18 years of age: the Pediatric AIDS Clinical Trials Group P1009 study. *J Allergy Clin Immunol* 112:973-980.

Table 1. Immunological characteristics of the patient.

Parameter	Patient		Normal range
Serum immunoglobulin			
IgM (g/L)	↓	0.23	0.4 – 2.5
IgG (g/L)	N / (↓) ^[a]	7.04	6.0 – 13.0
IgA (g/L)	N	2.75	0.8 – 3.0
IgE ^[b] (kU/L)	N	190	< 380
Leukocyte count (no./μL) and phenotype (%)			
Lymphocytes (/μL)	N	1170	1000 – 5300
CD19 ⁺ B cells			
CD19 ⁺ (/μL)	N	530	200 – 600
CD38 ⁺⁺ IgM ⁺⁺ transitional (%)	↑	14.2	4.6 – 8.3 ^[c]
CD27 ⁺ IgD ⁺ naïve (%)	↑	91	47.3 – 77.0 ^[c]
CD27 ⁺ IgD ⁺ natural effector (%)	↓	3.44	5.2 – 20.4 ^[c]
CD27 ⁺ IgD ⁻ switched memory (%)	↓	1.12	10.9 – 30.4 ^[c]
CD3 ⁺ T cells			
CD3 ⁺ (/μL)	↓	570	800 – 3500
CD4 ⁺ (/μL)	↓	180	400 – 2100
CD4 ⁺ CD45RA ⁺ naïve (%)	↓	39	46 - 77 ^[d]
CD4 ⁺ CD45RO ⁺ memory (%)	↑	61.1	13 - 30 ^[d]
CD4 ⁺ CD45RA ⁺ CD31 ⁺ RTE (%)	↓	32.5	42 - 74 ^[d]
CD8 ⁺ (/μL)	N	280	200 – 1200
CD8 ⁺ CD45RA ⁺ naïve (%)	↓	41.4	63 - 92 ^[d]
CD8 ⁺ CD45RO ⁺ memory (%)	↑	58.6	4 - 21 ^[d]
CD16 ⁺ CD56 ⁺ NK cells (/μL)	N	80	70 – 1200
Eosinophils (/μL)	↑	1150	< 350
TRECs (/10 ⁶ MNC)	↓	1197	> 10000
Specific IgG responses			
Tetanus toxoid (IU/ml)	N	0.03	> 0.01
Haemophilus influenza type b (μg/ml)	↓	< 0.15	0.15 – 1.0
Pneumococcal polysaccharides (U/ml)	↓	1	> 14
Measles	absent		
Varicella zoster	absent		
T cell proliferation			
PHA	↓ ↓ absent at 10 years of age ↓ decreased at 15 years of age		

N, value within normal range; ↑, value above normal range; ↓, value below normal range; RTE, recent thymic emigrants; TREC, T cell receptor rearrangement excision circle; PHA, phytohaemagglutinin

[a] Serum IgG dropped within a year after initial presentation.

[b] Serum IgE was measured after identification of the DOCK8 mutation on serum samples frozen before start of immunoglobulin replacement therapy.

[c] 5 – 95 percentile range for age-matched controls adopted from (7).

[d] 10 – 90 percentile range for age-matched controls adopted from (8).

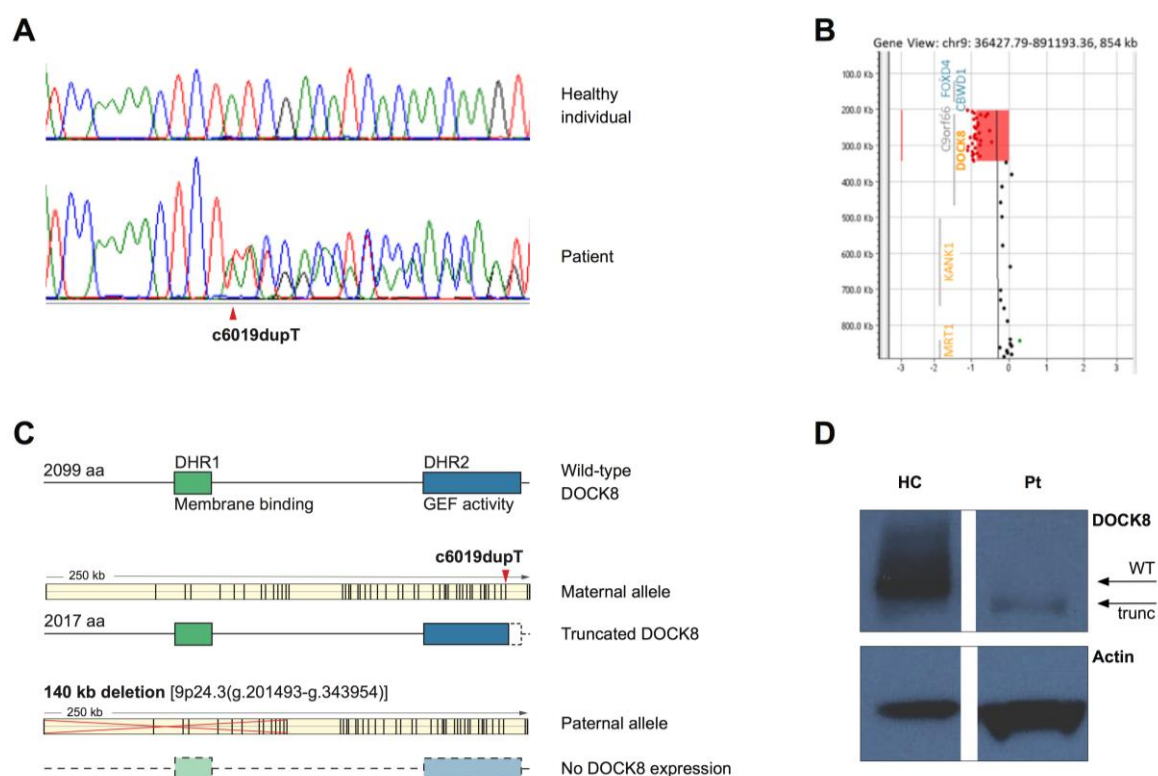
Figure 1

Figure 1. A novel compound heterozygous mutation in *DOCK8* results in expression of a truncated *DOCK8* protein. (A) Sanger sequencing results for the single nucleotide duplication, c.6019dupT, p.(Tyr2007Leufs*12). The upper panel illustrates a normal control trace and the lower panel shows the presence of the mutation; the duplicated T nucleotide is indicated by the arrow. (B) Results of array comparative genomic hybridization illustrating the about 140 kb deletion in 9p24.3 (204,193-343,954). The deletion encompasses exons 1-14 of *DOCK8*. (C) Graphic depicting the wild-type *DOCK8* protein structure and the outcome of the single-nucleotide insertion on the maternal allele and the deletion in *DOCK8* on the paternal allele on *DOCK8* protein expression (*DOCK8* transcript reference is ENST00000453981). (D) *DOCK8* protein expression in EBV-transformed B cells of a healthy control (7.5 µg protein lysate) and the patient (30 µg protein lysate). Actin was used as loading control.

Figure 2

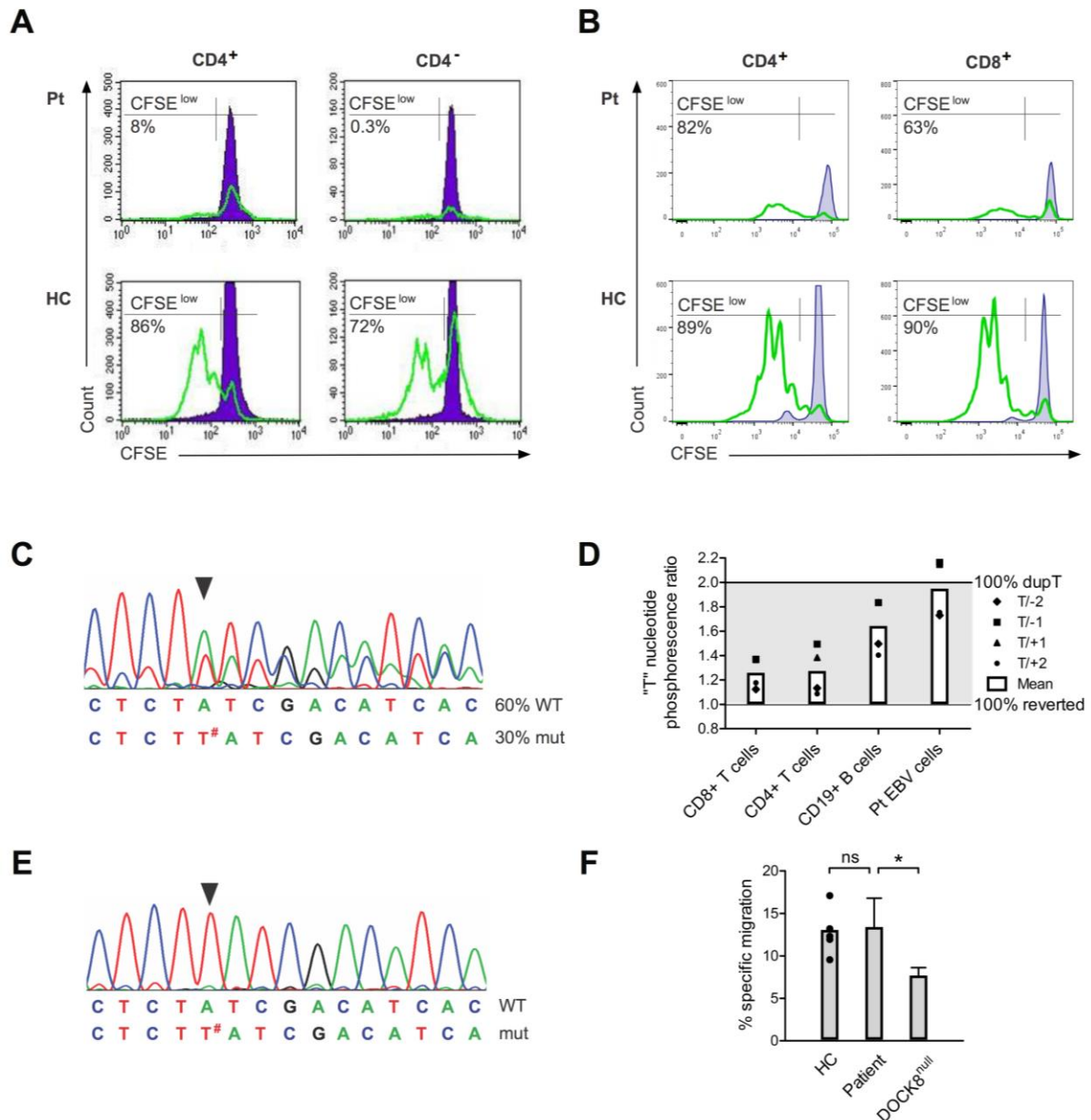


Figure 2. Improvement of T cell proliferation over time, somatic reversion of *DOCK8* in T cells and hypomorphic function of the truncated *DOCK8* protein. Proliferation of PHA-stimulated, CFSE-labeled PBMCs of the patient at (A) 10 and (B) 15 years of age, and a healthy control. Depicted are percentages of CFSE^{low} cells gated on CD3⁺ CD4⁺ or CD4⁻ or CD8⁺ T cells. (C) Sanger sequence trace showing somatic reversion of the single nucleotide

duplication (c.6019dupT) resulting in expression of about 60% wild-type *DOCK8* transcripts in the patient's CD3⁺ T cells. **(D)** "T" nucleotide phosphorescence ratios obtained by pyrosequencing *DOCK8* of primary CD3⁺CD4⁺ and CD3⁺CD8⁺ T cells, primary CD19⁺ B cells and the EBV B cell line of the patient. (T / \pm 1 or 2) depicts the signal ratio of c.6018-19T to nucleotides 1 and 2 positions up and downstream. The PCR templates and pyrosequencing reactions were performed in triplicate. Each symbol represents the mean of the three ratio measurements at respective nucleotide positions. The bar represents the mean "T" nucleotide phosphorescence ratio of all 4 different nucleotide ratios in indicated cell populations. **(E)** Sanger sequence trace showing expression of solely mutated *DOCK8* transcripts in EBV-transformed B cells of the patient. The duplicated T-nucleotide is indicated by the arrow and #. **(F)** Migration of EBV-transformed B cells of 5 different healthy controls (each symbol represents the mean of 3 independent experiments for each of the healthy control samples), the patient and a patient with a complete loss-of-function mutation in *DOCK8* (*DOCK8*^{null}). The bar of the healthy control samples represents the mean of the mean of each of the 5 healthy control samples. The bar for each of the patient samples represents mean and standard deviation of 3 independent experiments for each sample.

SUPPLEMENTARY DATA

METHODS

Study approval

Anticoagulated peripheral blood samples were obtained from the patient, her parents and healthy individuals after the provision of informed, written consent.

The patient and parents gave written consent (12/SC/0044) and the studies were performed according to the Declaration of Helsinki.

The parent-child trio were consented for exome sequencing; however, their consent was restricted to genes related to their condition and not for whole exome sequence (WES) analysis. Consequently, the patients have not consented for all data generated by WES or array CGH to be publically available. Therefore, we are not able to provide WES data beyond the immune-related targeted analysis.

DNA isolation

DNA extraction was performed using the FlexiGene DNA kit (Qiagen) according to the manufacturer's instructions.

Flow cytometry

Immunophenotypes were determined using whole blood and standard protocols with mixtures of fluorochrome-conjugated mAbs and absolute count beads (TruCount, BD

Bioscience) according to manufacturer's instructions. To monitor lymphocyte proliferation, PBMCs were labeled with CFSE (carboxyfluorescein diacetate, succinimidyl ester; Molecular Probes) according to manufacturer's instructions. After six days, CFSE dilution and T cell phenotype was determined by flow cytometry with following antibodies: CD3 PerCP (SK7), CD3 Alexa Flour 700 (SK7), CD4 APC (SK3), CD4 Qdot605 (S3.5), CD8 Pacific Blue (3B5). Dead cell exclusion was performed with LIVE/DEAD® Fixable Aqua Dead Cell Stain Kit (life technologies).

Exome sequencing and analysis

Exome capture was performed using the NimbleGen SeqCap EZ Human Exome Library v2.0, according to the manufactures instructions, and sequenced using a 100 bp paired-end read protocol on an Illumina HiSeq. Approximately 15Gb of sequence were obtained for each of the three individuals (patient and parents), providing at least 10x vertical read depth over ~90% of the coding exome, as specified by the consensus coding sequence (CCDS) project. Reads were aligned to hg19 with Stampy (v1.0.20) (1) and variant calling of single nucleotide variants (SNVs) and short insertion and deletions (indels) was undertaken using Platypus (v0.5.2). (2) The variants were annotated and restricted to 200 immune related genes (IUIS list of PIDs (3)), using the Illumina VariantStudio data analysis software. Variants were initially filtered on a population frequency below 5% within the NHLBI GO Exome Sequencing Project (<http://evs.gs.washington.edu/EVS/>), which identified a single nucleotide duplication within *DOCK8*. Further scrutiny of SNVs within this gene identified two upstream SNPs (rs506121 and rs529208) that were homozygous in the patient and inherited from the mother who was heterozygous. A comparison of the mapped *DOCK8*

exonic read count for each individual suggested a paternally inherited deletion was present within the 5' region of this gene.

Genomic DNA sequencing

M13-tagged oligonucleotide primers targeting exon 47 of *DOCK8* (GenBank accession number: NM_203447.3) were used to amplify genomic DNA (Forward 5'-GACCACTGGAAGTAGCCCA-3'; Reverse 5'-TGCACTTTGAGAACCACTGC-3'). PCR products were amplified using Kappa 2G FAST DNA Polymerase (KAPA biosystems), according to the manufacturer's instructions, and purified using the Agencourt Ampure system (Beckman Coulter). Dideoxy Sanger sequencing was undertaken using universal M13 primers, BigDye Terminator kit 3.1 (Applied Biosystems), and purified using the Agencourt CleanSEQ system. Capillary electrophoresis was performed using an ABI Prism 3730 Genetic Analyser. cDNA numbering uses A for the initiating ATG as nucleotide 1 and the initiating ATG as codon 1. Sequence conservation of the DHR2 domain was analyzed in mutationtaster (www.mutationtaster.org).

Microarray-based comparative genomic hybridization (CGH)

Array CGH was performed on genomic DNA using the Agilent ISCA 8x60K array according to the manufacturer's protocol and scanned using an Agilent SureScan high resolution scanner. The position of the array targets was mapped to the UCSC genome browser release February 2009 (GRCh37/hg19). Data was analyzed using Agilent CytoGenomics 2.0 software package (genome build hg19) and restricted to the *DOCK8* locus on chromosome 9. The

absence of upstream probes prevented an accurate size estimate of the deletion (9p24.3 (204,193-343,954)), which encompasses exons 1-14 of *DOCK8*.

T cell proliferation

To analyze T cell proliferation 1×10^6 peripheral blood mononuclear cells (PBMCs)/ml were stimulated for six days with 2.5 µg/ml phytohaemagglutinin (PHA; Sigma-Aldrich) in RPMI-1640 medium supplemented with 10% FCS, 10 U/ml penicillin, 10 µg/ml streptomycin, 1 mM sodium pyruvate, 1% non-essential amino acids, 2 mM L-glutamine and 50 µM β-mercaptoethanol.

Generation of Epstein-Barr Virus (EBV)–immortalized B cell lines

Magnetic bead sorted CD19+ B cells (B cell isolation kit II, human, Miltenyi Biotec) were immortalized with Epstein-Barr-Virus-containing supernatant according to standard protocols.

Western Blot

Cell lysates were prepared using lysis buffer containing 50 mM Tris-HCl pH 8, 150 mM NaCl, 1 % NP-40 and Complete Protease Inhibitor (Roche). Incubation with antibodies specific for DOCK8 (H159, Santa Cruz Biotechnology) and β-actin (AC15, Sigma-Aldrich) was performed in PBS / 5 % non-fat milk / 0.1 % tween, followed by incubation with respective HRPO-coupled antibodies (Jackson ImmunoResearch or Sigma-Aldrich). Finally, membranes were incubated in SuperSignal West Pico Chemiluminescent Substrate (Thermo Scientific).

RNA extraction, reverse transcription, DOCK8-specific PCR and Sanger sequencing

RNA was extracted using TRIZOL reagent (Invitrogen) and quantified using the NanoDrop 1000 (Thermo Scientific). cDNA synthesis was performed with equal amount of RNA using SuperScript III reverse transcriptase (Invitrogen) and random hexamer primers (Amersham Pharmacia Biotech) according to standard protocols. DOCK8-specific PCR (transcript ID: ENST00000453981) was performed using Pfu DNA polymerase (Agilent Technologies), and the following primers and amplification program: Forward 5'-CATGAGCAGTACAGAAGGAACA-3' and reverse 5'-ACTGGGTTTCACATTCCTGAA-3', and 3 min at 95°C followed by 32 cycles consisting of 30 sec at 95°C, 30 sec at 58°C, and 45 sec at 72°C. After amplification, the DOCK8-specific PCR product was cleaned up using QIAquick PCR purification kit (Qiagen) and subjected to standard Sanger sequencing using DOCK8-specific primers listed beforehand. Sanger sequencing traces were visualized in Chromas (Technelysium Pty Ltd).

Peak height quantification in sequencing traces

To determine the percentage of wild-type and mutated *DOCK8* transcripts in respective cDNA samples, Sanger sequencing traces were subjected to quantitative analysis using the ab1 Peak Reporter tool (<http://apps.lifetechnologies.com/ab1peakreporter>). Ab1 sequencing files were converted into numerical peak height data of base traces by applying the 'ratio of maximal signals in a 7-scan window' calculation provided by the software. Subsequently, numerical peak height data were analyzed in Microsoft Excel. Percentages of wild-type and mutated *DOCK8* transcript sequences are depicted as the mean of the sequence contributing nucleotide percentages of the analyzed 20 nucleotide positions. Non

wild-type or non-mutated bases are called at a rate of about 5% which gives a total sequencing base call background of 10%.

Pyrosequencing

The c.6019dupT variant was detected in the separated cell population by pyrosequencing. PCR templates for pyrosequencing were amplified from cDNA (10 ng) using the biotinylated forward primer 5' TCCTGCTGATCCAAAAC 3' and reverse primer 5' GCCATTTTCCTTCTTACC 3'. Following PCR amplification, the biotinylated PCR products were placed in 96-well plates and bound to streptavidin-coated sepharose beads (GE Healthcare, Piscataway, NJ, USA). The PCR products were denatured, and the non-biotinylated fragments were washed from the beads using the Pyromark Q96 Vacuum Workstation (Qiagen). The beads were then resuspended in annealing buffer (40µL) containing 0.4 pmol of the sequencing primer (5' TCAACTTGTTGTGATGTCG 3'). Pyrosequencing was performed using the Pyro Gold Q96 reagents (Qiagen), using dispensations based on the target sequence with the Pyromark Q96 system. The PCR templates and pyrosequencing reactions were performed in triplicate. Raw data files were imported into excel for ratio calculations. "T" nucleotide phosphorescence signal ratios were calculated by dividing the phosphorescence signal of the "T" nucleotide at position c.6018-19 by the phosphorescence signals at 1 and 2 nucleotide positions up- and downstream of c.6018-19 (T/-1, T/+1, T/-2, T/+2). A reduced "T" nucleotide signal ratio indicates a lower mutational load which is equal to an increased rate of somatic reversion.

Transwell migration assay

Before transwell migration assays, EBV-transformed B cells were starved overnight in migration medium (RPMI-1640 supplemented with 0.25% fatty acid-free BSA (Sigma-Aldrich)). On the day of experiment, EBV cells (100 μ L of 2×10^6 cells/mL) in migration medium were added to the upper chamber of a Transwell (8 μ m pore size; Millipore). The lower chamber contained 600 μ L of migration medium enriched with 10% FCS. After 4 hours of migration at 37°C, cells from the lower chamber were collected, stained with DAPI (4',6-diamidino-2-phenylindole) for dead cell exclusion, and recorded on a flow cytometer (BD Fortessa) by timed acquisition. Specific migration was calculated as follows:

$$\text{specific migration} = \left[\frac{\# \text{ migrated cells} \times 100}{\# \text{ input cells}} \right] - [\text{migration at 0\% attractant}]$$

Statistics

Analyses were performed with PRISM software (GraphPad Software, Inc.). Statistical hypotheses were tested using the unpaired 2-tailed t test. Differences were considered significant if the P value was less than 0.05.

REFERENCES

1. Lunter, G., and Goodson, M. 2011. Stampy: a statistical algorithm for sensitive and fast mapping of Illumina sequence reads. *Genome Res* 21:936-939.
2. Rimmer, A., Phan, H., Mathieson, I., Iqbal, Z., Twigg, S.R., Consortium, W.G.S., Wilkie, A.O., McVean, G., and Lunter, G. 2014. Integrating mapping-, assembly- and haplotype-based approaches for calling variants in clinical sequencing applications. *Nat Genet* 46:912-918.
3. Al-Herz, W., Bousfiha, A., Casanova, J.L., Chapel, H., Conley, M.E., Cunningham-Rundles, C., Etzioni, A., Fischer, A., Franco, J.L., Geha, R.S., et al. 2011. Primary immunodeficiency diseases: an update on the classification from the international union of immunological societies expert committee for primary immunodeficiency. *Front Immunol* 2:54.